Computational Characterization of Sulfur−Oxygen-Bonded Sulfuranyl Radicals Derived from Alkyl- and (Carboxyalkyl)thiopropionic Acids: Evidence for σ*-Type Radicals

Dariusz Pogocki[†,‡] and Christian Schöneich*[,†]

Department of Pharmaceutical Chemistry, University of Kansas, 2095 Constant Avenue, Lawrence, Kansas 66047, and Institute of Nuclear Chemistry and Technology, Dorodna 16, 03-195 Warsaw, Poland

schoneic@ukans.edu

Received September 4, 2001

Sulfide radical cations are known to stabilize via sulfur−oxygen bond formation with carboxylic acid functions. However, structural information on the resulting sulfuranyl radicals has so far only been provided by ESR spectroscopy for more stable, aromatic-substituted species, while the rather short-lived aliphatic sulfuranyl radicals have largely been characterized by time-resolved UV spectroscopy only. Therefore, we have obtained theoretical structural information on S−O-bonded sulfuranyl radicals from three model compounds, *tert*-butyl 2-(methylthio)peroxybenzoate, 3-methylthiopropionic acid, and 3,3′-thiodipropionic acid, using density functional theory, semiempirical, and molecular mechanics methods. All S−O-bonded species exist predominantly as three-electron-bonded σ*-radicals with an estimated heterolytic bond dissociation energy of the S∴O bond on the order of 23−27 kcal mol^{-1}. Characteristic optical absorption bands, vibrational frequencies, and hyperfine coupling tensors are evaluated to facilitate the identification of such radicals by time-resolved UV, IR, and ESR spectroscopy.

Introduction

Sulfuranyl radicals are important intermediates in the one-electron oxidation of organic sulfides and methionine (Met),[1] which are preferred targets of reactive oxygen species.[2−6] Usually, the one-electron (1e) oxidation of sulfides leads to sulfide radical cations which can subsequently complex, preferentially intramolecularly, with oxygen-carrying substituents such as hydroxy, alkoxy, or carboxylate groups (reaction 1).[7−23]

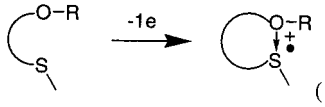

(1)

Evidence for a strong nonbonded attraction between sulfur and oxygen[24−27] in some biomolecules demonstrates that sulfur and oxygen can exist already at short distances from each other before oxidation, sometimes even at distances smaller than the sum of their respective van der Waals radii (3.3 Å).[28] The stabilization of 1e-oxidized sulfur through formation of sulfur−oxygen-bonded sulfuranyl radicals might potentially accelerate oxidation and autoxidation processes of substituted sulfides and of Met in peptides and proteins. For example, the electrochemical oxidation of dialkyl sulfides showed lower peak potentials when the sulfides were appended with neighboring carboxylate and alcohol groups.[29] Met oxidation is important during conditions of biological oxidative stress.[2,30−33] Specifically, the oxidation of Met[35]

* To whom correspondence should be addressed. Fax: (785) 864-5736.

† University of Kansas.

‡ Institute of Nuclear Chemistry and Technology.

(1) Schöneich, C.; Zhao, F.; Madden, K. P.; Bobrowski, K. *J. Am. Chem. Soc.* **1994**, *116*, 4641.

(2) Vogt, W. *Free Radical Biol. Med.* **1995**, *18*, 93.

(3) Pryor, W. A.; Jin, X.; Squadrito, G. L. *Proc. Natl. Acad. Sci. U.S.A.* **1994**, *91*, 11173.

(4) Pryor, W. A.; Squadrito, G. L. *Am. J. Physiol.* **1995**, *268*, L699.

(5) Moreno, J.; Pryor, W. A. *Chem. Res. Toxicol.* **1992**, *5*, 425.

(6) Hühmer, A. F. R.; Gerber, N. C.; Ortiz de Montelano, P. R.; Schöneich, C. *Chem. Res. Toxicol.* **1996**, *9*, 484.

(7) Perkins, C. W.; Martin, J. C.; Arduengo, A. J.; Lau, W.; Alegria, A.; Kochi, J. K. *J. Am. Chem. Soc.* **1980**, *102*, 7753.

(8) Glass, R. S.; Hojjatie, M.; Wilson, G. S.; Mahling, S.; Göbl, M.; Asmus, K.-D. *J. Am. Chem. Soc.* **1984**, *106*, 5382.

(9) Asmus, K.-D.; Göbl, M.; Hiller, K.-O.; Mahling, S.; Mönig, J. *J. Chem. Soc., Perkin Trans. 2* **1985**, 641.

(10) Chatgilialoglu, C.; Castelhano, A. L.; Griller, D. *J. Org. Chem.* **1985**, *50*, 2516.

(11) Mahling, S.; Asmus, K.-D.; Glass, R. S.; Hojjatie, M.; Wilson, G. S. *J. Org. Chem.* **1987**, *52*, 3717.

(12) Glass, R. S.; Petsom, A.; Hojjatie, M.; Coleman, B. R.; Duchek, J. R.; Klug, J.; Wilson, G. S. *J. Am. Chem. Soc.* **1988**, *110*, 4772.

(13) Bobrowski, K.; Holcman, J. *J. Phys. Chem.* **1989**, *93*, 6381.

(14) Mohan, H. *J. Chem. Soc., Perkin Trans. 2* **1990**, 1821.

(15) Chatgilialoglu, C. In *The Chemistry of Sulphenic Acids and Their Derivatives*; Patai, S., Ed.; John Wiley & Sons Ltd.: New York, 1990; pp 549−569.

(16) Steffen, L. K.; Glass, R. S.; Sabahi, M.; Wilson, G. S.; Schöneich, C.; Mahling, S.; Asmus, K.-D. *J. Am. Chem. Soc.* **1991**, *113*, 2141.

(17) Mohan, H.; Mittal, J. P. *J. Chem. Soc., Perkin Trans. 2* **1992**, 207.

(18) Schöneich, C.; Bobrowski, K. *J. Am. Chem. Soc.* **1993**, *115*, 6538.

(19) Bobrowski, K.; Schöneich, C. *J. Chem. Soc., Chem. Commun.* **1993**, 795.

(20) Marciniak, B.; Bobrowski, K.; Hug, G. L.; Rozwadowski, J. *J. Phys. Chem.* **1994**, *98*, 4854.

(21) Pogocki, D. Study on the hydroxyl radical induced reactions in amino acids and peptides containing thioether group. Ph.D. Thesis, Institute of Nuclear Chemistry and Technology, Warsaw, Poland, 1996.

(22) Bobrowski, K.; Hug, G. L.; Marciniak, B.; Miller, B. L.; Schöneich, C. *J. Am. Chem. Soc.* **1997**, *119*, 8000.

(23) Bobrowski, K.; Pogocki, D.; Schöneich, C. *J. Phys. Chem. A* **1998**, *102*, 10512.

(24) Burling, F. T.; Goldstein, B. M. *J. Am. Chem. Soc.* **1992**, *114*, 2313.

(25) Nagao, Y.; Hirata, T.; Goto, S.; Sano, S.; Kakehi, A.; Iizuka, K.; Shiro, M. *J. Am. Chem. Soc.* **1998**, *120*, 3104.

(26) Wu, S.; Greer, A. *J. Org. Chem.* **2000**, *65*, 4883.

(27) Reznik, R.; Greer, A. *Chem. Res. Toxicol.* **2000**, *13*, 1193.

(28) Bondi, A. J. *J. Phys. Chem.* **1964**, *68*, 441.

(29) Glass, R. S.; Hojjatie, M.; Petsom, A.; Wilson, G. S.; Göbl, M.; Mahling, S.; Asmus, K.-D. *Phosphorus Sulfur Relat. Elem.* **1985**, *23*, 143.

(30) Levine, R. L.; Mosoni, L.; Berlett, B. S.; Stadtman, E. R. *Proc. Natl. Acad. Sci. U.S.A.* **1996**, *93*, 15036.

10.1021/jo010894l CCC: $22.00
Published on Web 01/31/2002

in β-amyloid peptides (βAPs) 1−40 and 1−42, the major constituents of senile plaques in Alzheimer's disease, has been associated with part of the neurotoxicity of these sequences.[34,35] In the helical C-terminus of βAP 1−40, the stabilization of oxidized Met[35] through association with the C═O group of the peptide bond C-terminal to Ile[31] may be possible, as the ca. 3.6 Å average S−O distance between Met[35] and Ile[31] C═O in the native sequence[36] is close to the sum of the van der Waals radii of the two atoms.[28] In fact, we have recently obtained experimental evidence for such sulfide radical cation−amide association during the 1e oxidation of Met in the model compound *N*-acetylmethionine amide,[37] supporting the assumption that such a mechanism may promote Met oxidation in βAP.

The nature of S−O-bonded sulfuranyl radicals has been the subject of several investigations.[7,10,15,20,38−40] On the basis of semiempirical calculations, and parallel UV and ESR experiments, several bonding models have been proposed where the canonical ground-state electronic structures are of the π-, σ-, or σ*-type.[15] Despite experimental difficulties to discriminate between π-, σ-, and σ*-structures,[38] there is good evidence that the π-configuration is usually adopted by aryl-substituted sulfuranyl radicals. In such a structure the unpaired electron can be found on the orbital which is perpendicular to the plane defined by the sulfur and its three nearest neighbors. Its delocalization into the π-orbital of the benzene ring could be detected by ESR spectroscopy. The sulfuranyl radicals $(CF_3O)_3S^\bullet$, $(RO)_3S^\bullet$, and $(RO)_2S^\bullet F$ probably adopt a T-shaped configuration and can be described in terms of the σ-structure, in which the unpaired electron is localized in an orbital lying in the plane defined by the sulfur atom and its three nearest neighbors. On the other hand, in the σ*-structure, the configuration about the sulfur atom is pyramidal, and the transition from the σ- to the σ*-structure requires a conformational change from planar to pyramidal configuration around the sulfur atom. The radicals $CF_3SS^\bullet R_2$, $RC(O)SS^\bullet R_2$, and $(CH_3)_3SiOS^\bullet R_2$ have been assigned the σ*-type structure.[39,40] It has been suggested that σ*- and σ-type sulfuranyl radicals absorb in the 390 nm region whereas π-type sulfuranyl radicals absorb in the 340 nm region.[7,10,15,39,40] The experimental characterization of the more stable, aryl-substituted sulfuranyl radicals has been accomplished by ESR analysis. In contrast, time-resolved methods such as pulse radiolysis and laser flash photolysis connected to UV spectroscopy are the only techniques amenable to study the rather short-lived alkyl-substituted sulfuranyl radicals. Most pulse radiolytically observed sulfuranyl radicals have been arbitrarily assigned to the σ*-structure.[8−10,13−17] However, recently we have obtained kinetic evidence for at least two different sulfuranyl radicals, both absorbing with λ_{max} = 390 nm in the 1e oxidation of 3,3′-thiodipropionic acid.[23] Moreover, the absorbance maximum (λ_{max} = 390 nm) of sulfuranyl radicals from *endo*-6-(methylthio)bicyclo[2.21]heptane-*endo*-2-carboxylic acid is shifted to λ_{max} = 340 nm through incorporation of an additional amino group at the *exo*-2- position.[16] Therefore, multiple structures of aliphatic sulfuranyl radicals seem possible, and our objective in this paper is a detailed computational analysis of such structures to help to interpret results obtained by time-resolved techniques.

Radicals under Investigation. We have computationally investigated the geometry and the electronic composition of three model sulfuranyl radicals, **1**−**3**. Radical **1** is the product of low-temperature photolysis of *tert*-butyl 2-(methylthio)peroxybenzoate (**I**) (reaction 2),[7,10] and sulfuranyl radicals **2** and **3** are obtained

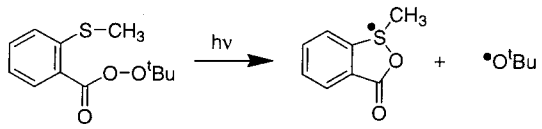

(2)

through the •OH-radical-induced oxidation of 3-methylthiopropionic (**II**) and 3,3′-thiodipropionic acids (**III**) (reactions 3 and 4), respectively.[23] We have chosen these radicals as their existence has been indicated through ESR,[7] pulse radiolysis,[11,14,23] and laser flash photolysis[10] experiments.

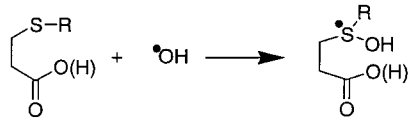

(3)

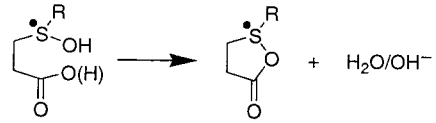

(4)

2 R = CH_3

3 R = $CH_2CH_2CO_2^-$

Computational Methods

See the Supporting Information.

Results

Radicals Derived from *tert*-Butyl 2-(Methylthio)-peroxybenzoate (I). Geometry. The geometry of radical **1** was optimized in the vicinity of the T-shaped (σ-sulfuranyl) MINDO-UHF structure, initially suggested by Kochi and co-workers,[7] by fully relaxed gas-phase B3LYP/(6-31G(d), 6-31+G(d), 6-311+G(d)) gradient minimization, and examined by the relaxed potential energy scan along the coordinate of the improper torsion angle $\angle_{O-S-C^2-CH_3}$, defined by the O−S−C^2 plane and the direction of the S−CH_3 bond. Both methods lead to

(31) Chao, C. C.; Ma, Y. S.; Stadtman, E. R. *Proc. Natl. Acad. Sci. U.S.A.* **1997**, *94*, 2969.
(32) Moskovitz, J.; Berlett, B. S.; Poston, J. M.; Stadtman, E. R. *Proc. Natl. Acad. Sci. U.S.A.* **1997**, *94*, 9585.
(33) Moskovitz, J.; Flescher, E.; Berlett, B. S.; Azare, J.; Poston, J. M.; Stadtman, E. R. *Proc. Natl. Acad. Sci. U.S.A.* **1998**, *95*, 14071.
(34) Butterfield, A. D. *Chem. Res. Toxicol.* **1997**, *10*, 495.
(35) Sayre, L. M.; Zagorski, M. G.; Surewicz, W. K.; Krafft, G. A.; Perry, G. *Chem. Res. Toxicol.* **1997**, *10*, 518.
(36) Coles, M.; Bicknell, W.; Watson, A. A.; Fairlie, D. P.; Craik, D. J. *Biochemistry* **1998**, *37*, 11064.
(37) Schöneich, C.; Pogocki, D.; Wisniowski, P.; Hug, G.; Bobrowski, K. *J. Am. Chem. Soc.* **2000**, *122*, 10224.
(38) Chanon, M.; Rajzman, M.; Chanon, F. *Tetrahedron* **1990**, *46*, 6193.
(39) Giles, J. R. M.; Roberts, B. P. *J. Chem. Soc., Perkin Trans. 2* **1980**, 1497.
(40) Morton, J. R.; Preston, K. F. *J. Phys. Chem.* **1973**, *77*, 2645.

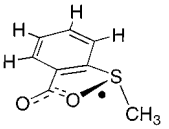

Figure 1. Structure of radical **1A(S)**. (The Cartesian coordinates are presented in the Supporting Information.)

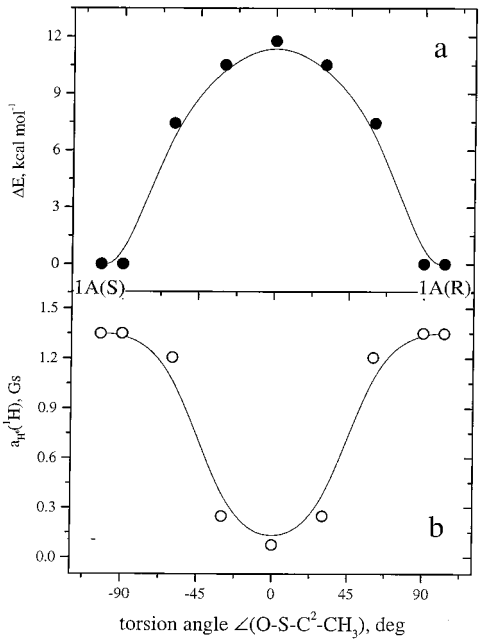

Figure 2. (a) Energy and (b) H^6 hydrogen hyperfine coupling tensor $a_{H6}(^1H)$ profile along the $\angle_{O-S-C^2-CH_3}$ coordinate for radical **1**, calculated on the $\mathscr{R}$-level.

structure **1A** of two enantiomeric radicals separated by a barrier of inversion of ca. 12 kcal mol^{-1}. One of the enantiomers, **1A(S)**, is shown in Figure 1. The energy profile along the $\angle_{O-S-C^2-CH_3}$ coordinate for radical **1** is shown in Figure 2a. Radical **1A** adopts a pyramidal σ^*-type S−O-bonded structure, which can be described approximately as a two-center, three-electron (2c, 3e) bond. In the $\mathscr{R}$-optimized structure ($\mathscr{R}$ refers to the B3LYP/6-31+G(d) level of theory and $\mathscr{R}1$ to the B3LYP/6-311+G(d) level; see the Computational Methods), the odd electron in **1A** is located in the σ^*-orbital, which is essentially an antibonding combination of the sulfur $3p_x$ orbital with the in-plane $2p_\sigma$ orbital of the carboxylate oxygen (the dihedral angle $\angle_{OCOS} \approx -179.9°$). The oxygen $2p_\sigma$ orbital, involved in the S−O bond, possesses partial sp^3 character, as seen from the $\angle_{COS}$ angle equal to 104.8° and the r_{C-OS} bond length equal to ca. 1.31 Å. Note that the bond length between the second oxygen and the carboxylic carbon, $r_{O=COS}$, is equal to ca. 1.23 Å. The calculated oxygen−sulfur bond lengths, r_{S-O}, vary only slightly with the extension of the basis set from 2.412 Å for 6-31G(d) to 2.388 Å for 6-31+G(d) and 2.389 Å for 6-311+G(d). (Also, the root-mean-square-distance (RMSD) of the Cartesian coordinates of all atoms in the $\mathscr{R}$- vs the $\mathscr{R}1$-optimized structures of **1A** was lower than 0.0113 Å.) The five-membered ring of **1A** is practically flat, since its flexibility is significantly limited by conjugation with the benzene ring. Thus, an energy profile for pseudorotational interconversion,[41−43] developed by sequential constriction of each one of the intraring dihedrals to planarity, shows the difference between **1A** and the "high-energy" conformers below 2.1×10^{-2} kcal mol^{-1}, while the intraring dihedral angles vary over a range narrower then 3.1°.

Spectral Properties. The vibrational frequency of **1A**, calculated through $\mathscr{R}$, amounts to $\omega_{SO} = 628.2$ cm^{-1} ($F = 2.26$ N cm^{-1}), which can be assigned to the S−O bond stretch. The extension of basis sets to 6-311+G(d) results in a very similar value of $\omega_{SO} = 631.6$ cm^{-1} ($F = 2.27$ N cm^{-1}). The proton hyperfine isotropic coupling constants, calculated with the B3LYP functional with the 6-31+G(d), 6-311++G(d,p), and EPR-III basis sets in the CPCM and the IEFPCM solvent models with $\epsilon = 8.93$ (CH_2Cl_2) at the $\mathscr{R}$-optimized geometry, show reasonable agreement with the values obtained experimentally by Kochi and co-workers.[7] Figure 2b shows the dependence of the hyperfine isotropic coupling constant of the aromatic proton H^6 calculated on the $\mathscr{R}$-level vs the improper torsion angle $\angle_{O-S-C^2-CH_3}$ in radical **1**. The best agreement with the experimental results was obtained for the enantiomers **1A(S)** and **1A(R)** (compare with data in Table 1). Also the TD-DFRT-calculated energy of the most intense one-electron transition (3.18 eV, 391 nm (//$\mathscr{R}$), 3.15 eV, 393.3 nm (//$\mathscr{R}1$)) corresponds well to the experimental results obtained by Chatgilialoglu and co-workers.[10] The calculated energy band is described essentially by a one-electron transition between the occupied σ and the singly occupied σ^* molecular orbitals, as evident from the weighting coefficient $c[\beta\rightarrow\beta^*] = 0.88$. The ZINDO/S calculation of the UV absorption has located the lowest electronic transition at 385 nm. The presence of the solvent (CH_2Cl_2) could not be included in UV absorption calculations due to the lack of chlorine atom parametrization in the ZINDO/S method. However, one can expect only a modest solvent effect on the position of the UV absorption band due to the moderate polarity of the solvent ($\epsilon = 8.93$),[44] and the small growth (ca. 4%) of the dipole moment of **1A** during excitation. In Table 1 we have summarized the calculated structural and spectral properties of radical **1A,** comparing them with the experimental data.

Radicals Derived from 3-Methylthiopropionic Acid (II). Gas-Phase Geometry. The initial structure for radical **2** derived from 3-methylthiopropionic acid was assembled by analogy to radical **1A(S)**. Conformational preferences in the cyclized species **2** were assessed by calculating a number of envelope structures in which each one of the intraring dihedral angles was sequentially constrained to be planar. Figure 3 displays an energy profile for pseudorotational interconversion.[41−43,45] Along the atoms S(0), O(1), C(2), C(3), and C(4) we obtain a double minimum pathway with valleys when carbon C(3) across the ring from the S−O bond is out of plane (conformers ^3E and E_3). The fully relaxed gas-phase geometry optimization in the vicinity of the constrained structures of the lowest energy led to two distinct

(41) Garrett, E. C.; Seranni, A. S. In *Computer modeling of carbohydrate molecules*; French, A. D., Brady, J. W., Eds.; American Chemical Society: Washington, DC, 1990; pp 91−119.
(42) Altona, C.; Geise, H. J.; Romers, C. *Tetrahedron* **1967**, *24*, 13.
(43) Altona, C.; Sundaralingam, M. *J. Am. Chem. Soc.* **1973**, *94*, 8205.
(44) Reichardt, C. *Solvents and Solvent Effects in Organic Chemistry*; VCH: Weinheim, 1988.
(45) Carmichael, I. *Acta Chem. Scand.* **1997**, *51*, 567.

Table 1. Structure and Properties of Radical 1A

	r_{SO} (Å)	ω_{SO} (cm^{-1})	F (N cm^{-1})	$\angle_{OCOS}$ (deg)	$a(^1H)$ (G) CH_3[a]	$a(^1H)$ (G) H^6	$a(^{33}S)$ (G)	$a(^{17}O)$ (G)	UV λ_{max} (nm)	f	$c[\beta \rightarrow \beta^*]$
Experiment											
					8.97[b]	1.46[b]			380−400[c]		
Calculation											
	2.389[d]	628.2[d]	2.26[d]	179.898[d]	7.33[f]	1.42[f]	18.51[f]	−23.48[f]	391,[g] 385[h]	0.12[g]	0.88 ($\sigma \rightarrow \sigma^*$)
	2.387[e]	631.6[e]	2.27[e]	179.93 1[e]	6.06[i]	1.46[i]	18.21[i]	−24.57[i]	393[j]	0.11[j]	0.88 ($\sigma \rightarrow \sigma^*$)
					7.35[k]	1.53[k]	18.40[k]	−27.76[k]			
					7.28[l]	1.52[l]	18.42[l]	−27.59[l]			

[a] For the methyl group, an average value for the static orientation of the three hydrogens is presented. [b] Generated by low-temperature photolysis of *tert*-butyl 2-(methylthio)peroxybenzoate in methylene chloride solutions. Reference 7. [c] Generated by low-temperature photolysis of *tert*-butyl 2-(methylthio)peroxybenzoate in methylene chloride solutions. Reference 10. [d] $\mathscr{R}$. [e] $\mathscr{R}1$. [f] CPCM(ϵ=8.93)-$\mathscr{R}$)//$\mathscr{R}$ and CPCM(ϵ=8.93)B3LYP/6-311++G(d,p)//$\mathscr{R}$. [g] TD-DFRT-$\mathscr{R}$//$\mathscr{R}$. [h] ZINDO/S//$\mathscr{R}$. [i] B3LYP/EPR-III[$]//$\mathscr{R}1$. [j] TD-DFRT-$\mathscr{R}1$//$\mathscr{R}1$. [k] CPCM($\epsilon$=8.93)-B3LYP/EPR-III[$]//$\mathscr{R}1$. [l] IEFPCM(ϵ=8.93)-B3LYP/EPR-III[$]//$\mathscr{R}1$.

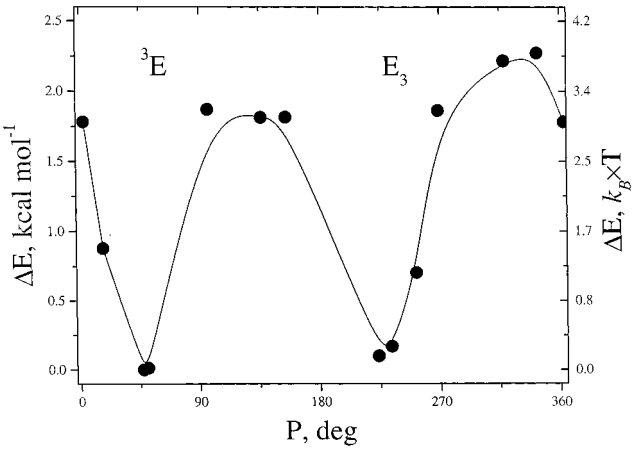

Figure 3. Energy profile along the pseudorotational interconversion of radical **2** calculated on the $\mathscr{R}$-level. *P* is the "phase angle" defined by the equation $tgP = ((\nu_4 + \nu_1) - (\nu_3 + \nu_0))/(2\nu_2(\sin 36° + \sin 72°))$, where ν_0, ν_1, ν_2, ν_3, and ν_4 are the torsion angles of a pentacyclic ring (ν_0 = C(4)−S(0)−O(1)−C(2); ν_1 = S(0)−O(1)−C(2)−C(3); ν_2 = O(1)−C(2)−C(3)−C(4); ν_3 = C(2)−C(3)−C(4)−S(0); ν_3 = C(3)−C(4)−S(0)−O(1)).[42,43]

stable conformers, **2A** and **2B**, which are denoted "^{3}E" and "E_3" after the envelope forms from which they are derived.

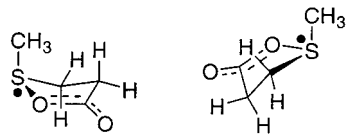

2A(^{3}E) **2B**(E_3)

These conformers are very close in energy with the **2B**(E_3) structure lying about 0.1 kcal mol^{-1} below the **2A**(^{3}E) form. The interconversion between ^{3}E end E_3 requires an energy of ca. 1.75−2.25 kcal mol^{-1}, equivalent to ca. 3−3.8 units of thermal energy at 298 K (k_BT; see Figure 3). (Calculations using the CPCM, IEFPCM, and MST methods showed that the height of the conversion barrier is similar to that in water.) Both low-energy conformers ^{3}E end E_3 adopt the pyramidal σ*-type arrangement with the odd electron on the σ*-orbital, an antibonding combination of the sulfur $3p_x$ orbital and the in-plane $2p_\sigma$ orbital of the oxygen of the carboxylate group (the dihedral angle $\angle_{OCOS} \approx -177.9°$ for **2A** and 160.0° for **2B**). Similarly to that of radical **1A,** the oxygen $2p_\sigma$ orbital of **2A** and **2B**, involved in S−O bond formation, possesses partial sp^3 character, as evident from the $\angle_{COS}$ angle equal to 105.8° for **2A** and 104.7° for **2B**, and the r_{C-OS} bond length equal to ca. 1.31 Å; instead, the length of the bond connecting the second oxygen with the carboxylate carbon, $r_{O=COS}$, is equal to ca. 1.23 Å in both conformations. The electronic structures of **2A** and **2B** can be approximately described as 2c, 3e, with the computed oxygen−sulfur bond lengths r_{S-O} being 2.410 Å for **2A** and 2.415 Å for **2B**.

Spectral Properties. The energies of the most intense one-electron transitions (**2A**, 3.03 eV, 410 nm; **2B**, 3.05 eV, 406 nm), calculated by TD-DFRT, are in good agreement with previous experimental results (see Table 2).[15,23] The calculated energy band is essentially described by a one-electron transition between the occupied σ and the singly occupied σ* molecular orbitals, as evident from the weighting coefficients displayed in Table 2. ZINDO/S calculations of the UV absorption have located the lowest electronic transition for **2A** and **2B** at 424 and 432 nm, respectively. Both conformers exhibit vibrational frequencies of ca. 546 cm^{-1}, which can be assigned to the S−O bond stretching mode.

Water-Phase Geometry. The CPCM (ϵ =78.4) reoptimization of **2A** and **2B** results only in a small deformation of the gas-phase structures. (The RMSDs of the Cartesian coordinates of atoms in radicals **2A** and **2B** vs their solvated forms **2A′** and **2B′** are summarized in Table 1S; see the Supporting Information) The obtained water-phase structures **2A′** and **2B′** are characterized by r_{S-O} = 2.390 Å, $\angle_{OCOS} \approx -178.2°$, and $\angle_{COS}$ = 105.5° for **2A′** and r_{S-O} = 2.389 Å, $\angle_{OCOS} \approx -179.2°$, and $\angle_{COS}$ = 104.6° for **2B′**.

Alternative Structures. During fully relaxed gas-phase energy minimization in the vicinity of a hypothetical T-shaped, σ-type, S−O-bonded structure (analogous to the MINDO-UHF structure[7] of radical **1**), radical **2** ultimately collapses to the pyramidal σ*-sulfuranyl radical **2A**. Similarly, during fully relaxed water-phase energy minimization (CPCM (ϵ =78.4)) in the vicinity of a hypothetical T-shaped σ-type structure, radical **2** collapses into the pyramidal σ*-sulfuranyl radical **2A′**.

An additional minimization attempt was done in the vicinity of a second hypothetical structure of the σ*-type sulfuranyl radical. In the planar local symmetry, the out-of-plane $2p_\pi$ orbitals of the carboxylate anion could potentially be involved in the formation of an S−O bond. The fully relaxed $\mathscr{R}$-gas-phase energy minimization of radical **2** in the vicinity of a hypothetical σ*-type $3p_{x-}2p_\pi$ structure leads to ring opening. The minimized structure **2C** is a sulfur-centered radical cation (>$S^{\bullet+}$) with the unpaired electron localized on the $3p_x$ SOMO orbital of

Table 2. Structure and Spectral Properties of Radicals 2A−2B′

configuration	r_{SO} (Å)	ω_{SO} (cm^{-1})	F (N cm^{-1})	$\angle_{O-C-O-S}$ (deg)	UV λ_{max} (TD-DFRT) (nm)	$\Delta\mu_{exc}$[d] (%)	f	$c[\beta \rightarrow \beta^*]$	UV λ_{max} (semiempirical) (nm) ZINDO/S	AM1	$\Delta UV_{s\ olv}$, λ_{max} (mixed calculation)[e] (nm) ZINDO/S	AM1
Experiment					410 (ϵ = 3200 $M^{-1}\,cm^{-1}$)[a] 390 (ϵ = 2500 $M^{-1}\,cm^{-1}$)[b]							
Calculation												
2A	2.410	545.7	0.72	−177.9	410[c]	5.52	0.16	0.88 ($\sigma \rightarrow \sigma^*$)	424	444	−70	−57
2B	2.415	546.3	0.86	160.0	406[c]	0.01	0.16	0.86 ($\sigma \rightarrow \sigma^*$)	432	463	−89	−6
2A′	2.390			−178.2								
2B′	2.389			−179.2								

[a] Reference 15. [b] Reference 23. [c] TD-DFRT-$\mathscr{R}//\mathscr{R}$. [d] Estimated change of the dipole moment μ during the excitation (see the text). [e] $\Delta UV_{solv} = \lambda_s - \lambda_g$ (see the text).

the thioether sulfur. The sulfur atom in **2C** is separated from the nearest oxygen by ca. 3.76 Å.

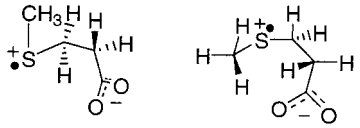

2C **2D'**

A TD-DFRT calculation shows that radical **2C** should not significantly absorb in the near-UV/vis region. The fully relaxed water-phase energy minimization (CPCM (ϵ =78.4)) of radical **2** in the vicinity of the hypothetical σ^*-type $3p_x$–$2p_\pi$ structure gives the less-extended structure of the radical cation (**2D′** (> $S^{\bullet+}$)), with the unpaired electron localized on the $3p_x$ SOMO orbital of the thioether sulfur, which is separated from the nearest oxygen by ca. 3.35 Å. Both gas-phase (**2C**) and water-phase (**2D′**) optimized structures of the sulfur-centered radical cation seem to be stabilized by the electrostatic attraction between the negatively charged carboxylate group and the cationic sulfur. Structure **2D′** describes a transient en route the experimentally observed[23] irreversible deprotonation in the α-position of the sulfur-centered radical cation that may actually be assisted by the carboxylate group (reaction 5).

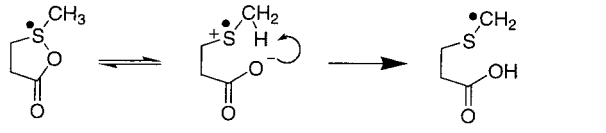

2 **2D'** (5)

All calculated structural and spectroscopic parameters of radicals **2A**−**2D′** are compared with the available experimental data in Table 2.

Radicals Derived from 3,3′-Thiodipropionic Acid (III). Geometry. The geometries of the S−O-bonded radical **3** derived from 3,3′-thiodipropionic acid were computed on the basis of assumed similarities with the geometries of radicals **2A** and **2B**, derived from 3-methylthiopropionic acid. Thus, in initial structures of radical **3,** prior to optimization, one of the propionic acid chains was "frozen" in the conformation corresponding to the ^3E or E_3 envelope in radical **2**. The second one, which substitutes the methyl group of **3**, was optimized on the B3LYP/3-21G(d) level, starting from local minima of the potential energy obtained by a scan performed on the AM1 level, along the coordinate of the $\angle_{C^3-S-C^{3\prime}-C^{2\prime}}$ torsion angle. Finally, after removal of all constraints, the molecules were freely optimized on the $\mathscr{R}$-level.

Our previous experimental results showed the presence of a S−O-bonded radical of 3,3′-thiodipropionic acid over the entire pH range between 1 and 7.[23] Thus, on the basis of known pK_a values of 3,3′-TDPA, 3.9 and 4.67,[46] we took into account the possibility of formation of the S−O-bonded structure of 3,3′-TDPA with the second carboxylate group protonated. The calculation procedure leads to structures **3A**−**3D**, and their respective protonated forms, **3AH**−**3DH**, shown in Figure 4 (the properties of radicals **3A**−**3DH** are summarized in Table 3; the respective Cartesian coordinates are presented in the Supporting Information).

Spectral Properties. The TD-DFRT-$\mathscr{R}$ calculation for the singly S−O-bonded radicals **3B**, **3C**, **3AH**, **3BH**, **3CH**, and **3DH** show the most intensive absorption band in the 400−450 nm region, which is 30−50 nm red-shifted compared to the experimental data obtained by pulse radiolysis (see Table 3).[15,23] Calculation for the O−S−O-bonded radicals **3A** and **3D** predicts an absorption band with maxima located at ca. 600 nm. Under normal experimental conditions,[14,23] such an absorption, if it exists, will overlap with that of other radical intermediates, e.g., with the low-energy shoulder of the absorption of a sulfur−sulfur-bonded dimeric radical cation.[15] Similar to those for radicals **1** and **2,** the calculated energy bands consist mainly of a $\sigma \rightarrow \sigma^*$ one-electron transition (see the weighting coefficients in Table 3). The semiempirical CI calculations show acceptable agreement with the TD-DFRT results with average discrepancies of 6.4% and 9.7% for the AM1 and ZINDO/S methods, respectively. The vibrational frequencies, which can be assigned to the S−O bond stretching mode are in the 541.1−572.6 cm^{-1} waveband, with the higher energy edge occupied by the O−S−O-bonded systems **3A** and **3D** and the intramolecularly H-bonded structure **3BH**.

Water-Phase Geometry. Each of the gas-phase-optimized structures presented in Figure 4 has its water-phase (CPCM-minimized) counterpart (referred to in the Supporting Information as structures **3A(H)′**∠**3D(H)′**). The respective RMSDs of the Cartesian coordinates of all atoms in the $\mathscr{R}$- vs CPCM-$\mathscr{R}$-minimized structures vary in the range from 0.03 to 0.32 Å (details are presented in Table 1S). Importantly, the solvation of

(46) Smith, R. M.; Martel, A. E. *Critical stability constants*; Plenum Press: New York, 1974.

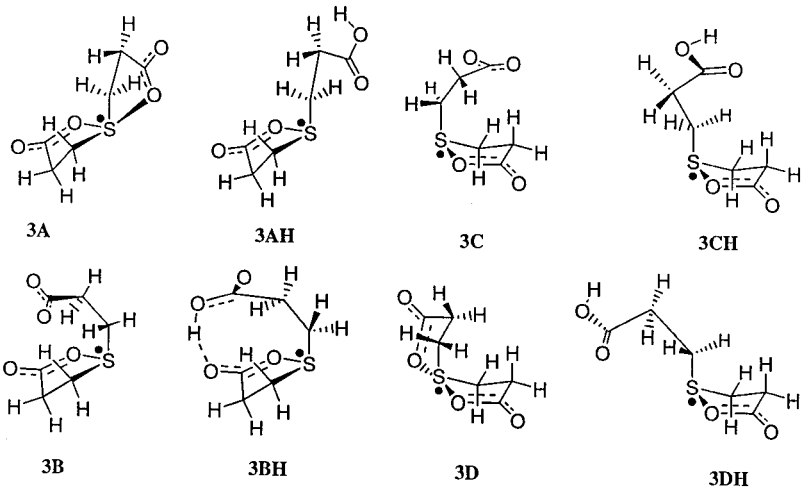

Figure 4. Structures of radicals **3A**−**3DH** obtained from the calculated Cartesian coordinates (presented in the Supporting Information) and insignificantly adapted to clarify the picture.

Table 3. Structure and Spectral Properties of Radicals 3A−3DH

configuration		r_{SO} (Å)	ω_{SO} (cm^{-1})	F (N cm^{-1})	UV λ_{max} (TD-DFRT) (nm)[b]	$\Delta\mu_{exc}$[c] (%)	f	$c[\beta\rightarrow\beta^*]$	UV λ_{max} (semiempirical) (nm) ZINDO/S	AM1	$\Delta UV_{s\,olv}$, λ_{max} (mixed calculation)[d] (nm) ZINDO/S	AM1
Experiment												
					∼350−420[a]							
Calculation												
3A	E_3	2.561	572.6	0.78	598	943	0.15	0.66 ($\sigma_2\rightarrow\sigma^*$)	624	576	−20	21
		2.563						0.42 ($\sigma_1\rightarrow\sigma^*$)				
3B	E_3	2.445	556.9	0.76	430	10.9	0.15	0.63 ($\sigma\rightarrow\sigma^*$)	374	431	29	42
								0.60 ($n\rightarrow\sigma^*$)				
3C	^3E	2.422	558.5	0.71	442	−6.54	0.13	0.87 ($\sigma\rightarrow\sigma^*$)	362	431	−1	5
3D	^3E, ^3E	2.611	572.4	0.77	599	493	0.22	0.73 ($\sigma\rightarrow\sigma^*$)	656	576	23	−3
		2.611						0.48 ($n\rightarrow\sigma^*$)				
3AH	E_3	2.416	554.5	0.86	411	4.98	0.18	0.87 ($\sigma\rightarrow\sigma^*$)	370	443	−43	9
3BH	E_3	2.394	570.1	1.08	404	−50.1	0.10	0.85 ($\sigma\rightarrow\sigma^*$)	392	371	−51	69
3CH	^3E	2.400	544.0	0.74	410	10.3	0.13	0.89 ($\sigma\rightarrow\sigma^*$)	367	447	−8	−36
3DH	^3E	2.403	541.1	0.71	403	9.46	0.18	0.89 ($\sigma\rightarrow\sigma^*$)	366	445	29	−60

[a] A broad area devoid of a structure band has been observed.[23] [b] TD-DFRT-*RII/R*. [c] Estimated change of the dipole moment μ during the excitation (see the text). [d] $\Delta UV_{solv} = \lambda_s - \lambda_g$ (see the text).

radicals **3B**, **3C**, **3AH**, and **3BH** leads to a small (0.02−2.6%) decrease of r_{SO}. Only in two cases, **3C** and **3BH**, is the solvation process accompanied by a decrease of the dipole moment of the molecule. For the remaining structures an increase of μ is observed. The calculated effects of solvation are presented in Table 1S.

The results of the ZINDO/S and AM1 mixed-model calculation of the solvatochromic shift of the UV absorption, which are summarized in the last two columns of Table 3, are highly inconsistent and, as such, cannot be used for the estimation of actual solvent effects.

Discussion

Nature of the Sulfur−Oxygen Bond. The most important result of our work is that all the density functional theory (DFT)-calculated structures are characterized by two-center, three-electron ($2\sigma/1\sigma^*$) bonds. Especially for radical **1**, these results contradict the interpretation of the ESR experiment performed by Kochi and co-workers.[7] In their work,[7] the ESR spectrum of the *tert*-butyl 2-(methylthio)peroxybenzoate-derived radical **1** has been interpreted in terms of a T-shaped σ-type S−O-bonded structure in agreement with MINDO-UHF calculations. The σ-type bonding scheme of radical **1** requires the methyl carbon to be approximately collinear with the S−O bond and coplanar with the aromatic ring, with the singly occupied MO primarily composed of σ-bonds in what has been termed a three-center, three-electron (3c, 3e) bond. However, in the DFT-calculated geometries the sulfur-bonded methyl group is almost perpendicular (ca. 89.6°) to the surface defined by the benzene ring and the carboxylate group. This strong support of a σ^*-bonded structure of radical **1** is significant since, up to now, the MINDO-UHF structure of **1,** proposed by Kochi and co-workers,[7] has been the only experimentally observed example reported for a σ-bonded sulfuranyl radical involving the participation of a carboxylate group.[47] Thus, considering all available data, it appears that S−O-bonded sulfuranyl radicals are electronically best described as two-center, three-electron S∴O-bonded.[48]

However, we need to take into account calculations of the $[H_2OSH_2]^{\bullet+}$ complex, reported by Carmichael.[49] He pointed out that a Mulliken population analysis of the electron charge and spin distribution based on the

(47) Hudson, A. *R. Soc. Chem. Spec. Period. Rep.* **1982**, *7*, 41.
(48) Gilbert, B. C. *R. Soc. Chem. Spec. Period. Rep.* **1982**, *7*, 174.
(49) Carmichael, I. *Nukleonika* **2000**, *41*, 11.

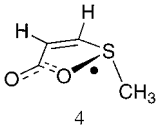

4

Figure 5. Structure of model radical **4**.

QCISD[50] density indicates that the unpaired spin resides mainly on the sulfur center, suggesting that this species is better described as a sulfuranyl radical. To relate our results to those of Carmichael, we have performed a series of single-point calculations introducing electron correlation by employing the second-, third-, and fourth-order Møller−Plesset correlation energy correction[51] (MP2,[52−56]MP3,[57,5857−58] MP4(SQD)[59,60]) and the quadratic configuration iteration theory limited to single and double excitation (QCISD).[50] The BH&HLYP functional, which includes 50% Hartree−Fock exchange, 50% Slater exchange, and additional correlation for effects of the LYP functional,[61] has also been included because of its fortuitous cancellation of errors for some three-electron-bonded radicals.[62] The spin densities calculated for model radical **4** (shown in Figure 5), which is related to the geometry of radical **1A** with the $\mathscr{R}$1-optmized vinyl protons, are summarized in Table 2S (see the Supporting Information). The collected results do not indicate underestimation of spin density by the DFT methods compared to the correlation methods; on the contrary, the spin population on the sulfur atom appears to be overestimated by DFT.

Estimation of the Sulfur−Oxygen Bond Energy. The direct calculation of the heterolytic bond dissociation energy of the S∴O bond in the intramolecularly bonded systems is difficult, due to the inability to completely separate the reactive centers, i.e., the sulfur-centered radical cation and the carboxylate anion. However, this energy can be estimated on the basis of simple assumptions which are illustrated in Figure 6, and briefly summarized below. To obtain a thermodynamically stable cyclic radical, the energy of the intramolecular S∴O bond, E_B, has to exceed, at least, the ring strain, E_R. Thus, E_B should be higher than the difference of the strain energy between the cyclic (S∴O-bonded) and the expanded structure of the radical. The fraction of the S∴O bond energy which is in excess over the minimum energy required for compensation of the ring strain, referred to as the stabilization energy (ΔE_{St}), is manifested by the difference in the energy between the cyclic and the expanded structures. The exact values of ΔE_{St} for each of the cyclic conformers of radical **2** can be calculated by subtraction of the $\mathscr{R}$-calculated energy (electronic + zero-point energy) of the expanded radical **2C** from the respective energies of radicals **2A** and **2B**. Such a calculation gives $\Delta E_{St} \approx -5.41$ and -5.44 kcal mol^{-1} for radicals **2A** and **2B,** respectively. On the other hand, the differences of the conformational energies between cyclic radicals **2A** and **2B** and the extended radical **2C** can be estimated by force field methods such as CHARMM or AMBER, which are generally utilized to reproduce experimental (or ab initio) molecular geometries and relative conformational energies.[63] Hence, we are able to calculate the differences in the conformational energies (strain energy) of radicals **2A**, **2B,** and **2C** by performing single-point CHARMM and AMBER molecular mechanics calculations. Importantly, the geometries and charge distributions of the respective radicals have been taken from DFT calculations. The CHARMM and AMBER single-point calculations of **2A**, **2B**, and **2C** report similar values of relative conformational energies, $\Delta E_{\mathbf{2A-2C}} = 19.3$ and $\Delta E_{\mathbf{2B-2C}} = 20.5$ kcal mol^{-1} by CHARMM, $\Delta E_{\mathbf{2A-2C}} = 17.6$ and $\Delta E_{\mathbf{2B-2C}} = 19.5$ kcal mol^{-1} by AMBER. Thus, keeping in mind the potential error of both molecular mechanics methods, we locate the energy of cyclization, E_R, of radical **2** in the range of 17−21 kcal mol^{-1}. Addition of the estimated energy of stabilization ($E_{St} \approx 6$ kcal mol^{-1}) to E_R gives an approximate value for the S∴O bond energy in the range of 23−27 kcal mol^{-1}. The obtained value exceeds the S∴O bond dissociation energy of $Me_2S\therefore OH_2^+$ (16.8 kcal mol^{-1}) calculated by Clark.[64] However, he has suggested this value as a low-energy limit for the weakest observable three-electron-bonded complexes in aqueous solution. In general S∴O bond dissociation energies appear lower than those of three-electron bonds between identical atoms, e.g., S∴S bonds, due to an inverse correlation between three-electron bond dissociation energies and the difference of ionization potentials of the bond-forming groups.[65] Gas-phase calculations predict low bond dissociation energies especially for overall neutral three-electron-bonded systems (pertaining to our sulfide radical cation−carboxylate complexes). However, Clark pointed out that such bonds will be strongly stabilized in solution.[65] We have experimen-

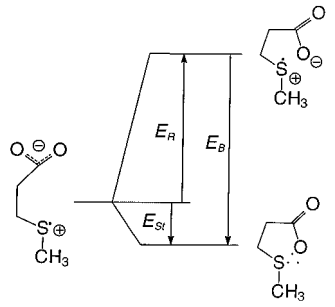

Figure 6. Graphical representation of the combined methods employed for the estimation of the S∴O bond energy (see the text).

(50) Pople, J. A.; Head-Gordon, M.; Raghavachari, K. *J. Chem. Phys.* **1987**, *87*, 5968.
(51) Møller, C.; Plesset, M. S. *Phys. Rev.* **1934**, *45*, 618.
(52) Saebo, S.; Almof, J. *Chem. Phys. Lett.* **1989**, *154*, 83.
(53) Head-Gordon, M.; Head-Gordon, T. *Chem. Phys. Lett.* **1994**, *220*, 122.
(54) Frisch, M. J.; Head-Gordon, M.; Pople, J. A. *Chem. Phys. Lett.* **1990**, *166*, 281.
(55) Frisch, M. J.; Head-Gordon, M.; Pople, J. A. *Chem. Phys. Lett.* **1990**, *166*, 275.
(56) Head-Gordon, M.; Pople, J. A.; Frisch, M. J. *Chem. Phys. Lett.* **1988**, *153*, 503.
(57) Pople, J. A.; Seeger, R.; Krishan, S. *Int. J. Quantum Chem. Symp.* **1977**, *11*, 149.
(58) Pople, J. A.; Binkley, J. S.; Seeger, R. *Int. J. Quantum Chem. Symp.* **1976**, *10*, 1.
(59) Trucks, G. W.; Watts, J. D.; Salter, E. A.; Bartlett, R. J. *Chem. Phys. Lett.* **1988**, *153*, 490
(60) Trucks, G. W.; Salter, E. A.; Sosa, C.; Bartlett, R. J. *Chem. Phys. Lett.* **1988**, *147*, 188.
(61) Becke, A. D. *J. Chem. Phys.* **1993**, *98*, 1372.
(62) Braida, B.; Hiberty, P. C.; Savin, A. *J. Phys. Chem. A* **1998**, *102*, 7872.
(63) Leach, A. R. *Molecular modelling: principles and applications*; Longman: Harlow, England, 1996.
(64) Clark, T. In *Sulfur-Centered Reactive Intermediates in Chemistry and Biology*; Chatgilialoglu, C., Asmus, K.-D., Eds.; Plenum Press: New York, 1990; pp 13−18.
(65) Clark, T. *J. Am. Chem. Soc.* **1988**, *110*, 1672.

Table 4. Bond Lengths (Å) and Bond Energies (kcal mol^{-1}) of the S∴O-Bonded Radicals Derived from 3-Methylthiopropionic Acid in Comparison to the Literature Data Obtained for Different Three-Electron-Bonded Complexes

radical	$r_{S\therefore X}$[a]	bond energy[b]	method and literature
2A, **2B**	2.41	23−27[c]	this work
$H_2S\therefore OH_2^+$		20.2	HF/6-31G(d)[d]
		23.8	MP2/6-31G(d)[d]
	2.437		MP2/6-311G(2d,p)[e]
	2.418		B3LYP/6-311G(2d,p)[e]
	2.454		QCISD/6-311G(2d,p)[e]
$Me_2S\therefore OH_2^+$	2.88	16.8	HF/6-31G(d)[f]
$Me_2S\therefore OH$	2.05	9.3	MP2/6-31+G(2d)[g]
		8.7	QCISD(T)/6-31+G(2d,p)//MP2/6-31+G(2d)[g]
$Me_2S\therefore O_{peptide}$	2.48	22.7	G2(MP2-B3LYP)//6-31G(d)[h]
$H_2S\therefore SH_2^+$	2.89	42.8	BP86/TZ2P[i]
	2.78	44.4	PW91/TZ2P[i]
	2.73		MP2/6-311++G(2df,2pd)[i]
		19.5	HF/6-311++G(2df,2pd)[i]
		33.5	PMP2/6-311++G(2df,2pd)[i]
		30.0	CCSD/6-311++G(2df,2pd)[i]
		31.9	CCSD(T)/6-311++G(2df,2pd)[i]
	2.84		MP2/6-31(d)[j]
		19.9	HF/6-31G(d)[j]
		33.4	PMP2/6-31+G(2df,p)[j]
		32.6	PMP4/6-31+G(2df,p)[j]
$Me_2S\therefore SMe_2^+$	2.84		HF/6-31G(d)[j]
	2.80		MP2/6-31G(d)[j]
		29.2	ΔH^{576} PMP4/6-31+G(2df,p)//MP2/6-31G(d)[j]
$Et_2S\therefore SEt_2^+$	2.86		C_{2v} conformer, HF/6-31G(d)[j]
	2.87		C_2 conformer, HF/6-31G(d)[j]
		26.8	ΔH^{520}, PMP4/6-31+G(2df,p)//HF/6-31G(d)[j]
$H_2S\therefore NH_3^+$	2.46	26.4	HF/6-311G(d,p)[k]
	2.54	44.6	B3LYP/6-311G(d,p)[k]
	2.44	34.1	QCISD/6-311G(d,p)[k]
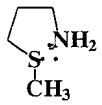	2.52		^{3}E conformer,HF/6-311G(d,p)[k]
	2.58		^{3}E conformer, B3LYP/6-311G(d,p)[k]
	2.54		E_3 conformer, HF/6-311G(d,p)[k]
	2.59		E_3 conformer, B3LYP/6-311G(d,p)[k]

[a] X = S, O, or N. [b] Bond dissociation energies of RS∴XR complexes in the scission into RS$^{\bullet+}$ and XR. [c] Estimation (see the text). [d] Reference 65. [e] Reference 49. [f] Reference 64. [g] Reference 66. [h] Reference 67. [i] Reference 68. [j] Reference 69. [k] Reference 45.

tally observed the absorption spectrum of $Me_2S\therefore OH$ (λ_{max} = 340 nm),[18] for which McKee[66] has calculated a significantly lower S∴O bond energy of ca. 9 kcal mol^{-1}. Our result is in qualitative agreement with the dissociation energy reported by Mahling et al.,[11] based on the temperature dependence of sulfur−carboxylate complex dissociation, from which they have predicted that the strength of the sulfur−carboxylate interaction exceeds that of $(>S\therefore OH_2)^+$ by about a factor of 2. The comparison of our estimation with literature data for other three-electron-bonded systems, shown in Table 4, indicates that the formation of a S∴O-bonded pentacyclic structure is thermodynamically attractive and can compete with other mechanisms of stabilization of sulfur-centered radical cations.

Especially interesting is the comparison with results for the analogous S∴N bond, formed between a sulfide radical cation and an amino group. On the basis of bond lengths and stretching frequencies for the S∴O bond (2.41 Å, 546 cm^{-1}), calculated for radical **2**, and the S∴N bond (2.52−2.59 Å, 224−263 cm^{-1}),[45] derived from 3-(methylthio)amine using the same B3LYP functional, we conclude that the sulfur−carboxylate S∴O bond must be stronger than the S∴N bond. This is especially so as the B3LYP procedure used for both the S∴O bond and the S∴N bond calculation appears to slightly overestimate the strength of three-electron bonds.[62] The stronger S∴O bond is not surprising taking into account the strong electrostatic attraction between a sulfur-centered radical cation and the carboxylate anion (ca. 15 kcal mol^{-1} based on the molecular mechanics estimation for **2A** and **2B**). Another practical aspect of the S∴O bond energy follows from its comparison with the energy of cyclization of *n*-alkanes to cycloalkanes.[70] The energy of the S∴O bond is higher than the enthalpy of cyclization of five- and higher-membered aliphatic rings. Thus, for such configurations the formation of a S∴O-bonded cycle should be thermodynamically allowed. This is in accordance with experimental results from others[8,9] and us[16,21,23] for several thioethers containing carboxylate functions. For instance, pentacyclic S∴O bonds have been observed for (carboxyalkyl)thiopropionic acid derivatives,[14,23] *S*-alkylcysteine derivatives,[9,21] and *S*-alkylglutathiones.[21] In addition, we observed hexacyclic S∴O bonds in methionine derivatives,[9,16,21] and heptacyclic S∴O bonds in homomethionine.[21] However, for larger rings (ring size ≥8 atoms), the S∴O-bonded structure can be significantly destabilized by a negative entropy of cyclization, which grows with the size of the ring.

Absorption Spectra of the Sulfur−Oxygen Bonds. For radicals **2** and **3**, but not radical **1**, the calculated

(66) McKee, M. L. *J. Phys. Chem.* **1993**, *97*, 10971.
(67) Rauk, A.; Armstrong, D. A.; Fairlie, D. P. *J. Am. Chem. Soc.* **2000**, *122*, 9761.
(68) Bickelhaupt, F. M.; Diefenbach, A.; de Visser, S. P.; de Konnig, L. J.; Nibbering, N. M. M. 1. *J. Phys. Chem. A* **1998**, *102*, 9533.
(69) Deng, Y.; Illies, A. J.; James, M. A.; McKee, M. L.; Peschke, M. *J. Am. Chem. Soc.* **1995**, *117*, 420.
(70) Isaacs, N. S. In *Physical Organic Chemistry*; John Wiley & Sons Ltd.: New York, 1987; pp 282−324.

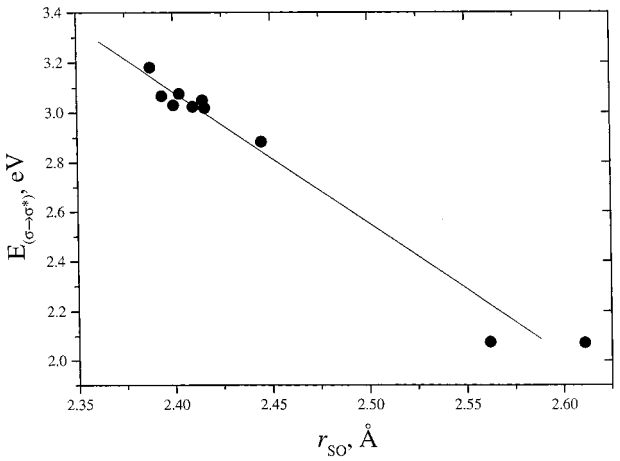

Figure 7. Variation of the TD-DFT-computed wavelengths of λ_{max} with the DFT-optimized S∴O bond length.

optical transitions are somewhat red-shifted compared to the experimental values obtained in water. However, this can be rationalized by the effect of water on the S∴O bond length, and hydrogen bonding of the respective radicals, as described below. The lowest energy optical band in all investigated radicals is assigned to a moderately strong $\sigma \rightarrow \sigma^*$ transition in the β-space. A useful quasi-linear relationship emerges on plotting the TD-DFT-calculated energy of the vertical transition against the $\mathcal{R}$-optimized length of the S∴O bond in radicals **1A, 2A, 2B, 3A, 3B, 3D**, and **3AH**−**3DH** (see Figure 7). The notable decrease of the energy of the $\sigma \rightarrow \sigma^*$ transition with the increase of the S∴O bond length is in accord with the intuitive interpretation of data for the S∴S bond,[71] which can be extended to the S∴O bond. The optical absorption energy of a three-electron bond should depend on the relative position of the σ- and σ^*-levels, and one parameter affecting the latter would be the extent of p orbital overlap. An increase of p overlap is associated with a lowering of the σ-level, and a rise of the σ^*-level, and, consequently, an increasing σ/σ^* separation. Thus, an increasing overlap should result in a blue shift and a decreasing overlap in a red shift of the absorption. Obviously, p overlap is expected to be a function of the internuclear distances, i.e., the bond lengths.

The relationship shown in Figure 7 allows an estimation of the change of λ_{max} as a function of r_{SO}. On the basis of the slope m of a plot of $E_{\sigma\rightarrow\sigma^*}$ vs r_{SO}, $m = -5.3$ eV Å^{-1}, we calculate that a 1% deviation of r_{SO} from $r_{SO} \approx 2.4$ Å for a S∴O-bonded radical absorption with λ_{max} ca. 400 nm will result in a shift of λ_{max} of ca. 17 nm. On the basis of this approach, a solvation-induced shortening of r_{SO} (see column 3 in Table 1S) results in a negative solvatochromic shift of ∼0.5−65 nm, bringing the computed absorption bands closer to those observed experimentally.[23] We can reasonably assume that, on the time scale of electronic excitation, the solvent geometry remains essentially fixed but not that of the solute. The solute's electrical properties, and, therefore, its van der Waals radius, change, as one expects the excited states with their more loosely held electron to be larger compared to the corresponding ground state. Thus, during excitation the solute has to absorb more energy to overcome the greater repulsion with the surrounding solvent. This effect should in general cause a blue shift.[72−74] A decrease of hydrogen bonding in the excited state will also cause a blue shift. For example, a significant blue shift was observed for the n $\rightarrow \sigma^*$ transitions of heteroatom-containing compounds, such as water, ammonia, hydrogen sulfide, and phosphine,[75] on going from a nonprotic to a protic medium. A similar situation applies to the investigated radicals. Their σ-levels possess partial n character due to the mixing of the σ-orbital with bonding and antibonding combinations of doubly occupied orbitals of lone pairs from the sulfur and the carboxylate oxygen. Thus, excitation promoting the electrons to the σ^*-level will decrease the electron density on the n orbitals, thereby reducing their nucleophilicity and ability to form hydrogen bonds. On the other hand, on the basis of the estimated growth of the dipole moment during excitation (see column 6 in Tables 2 and 3), a strongly polar medium (water) should cause a positive solvatochromic shift due to better stabilization of the more polar excited state compared to the less polar ground state.[76] Not unexpectedly, the semiempirical methods have only limited application to the problems of solvatochromic effects. They almost completely failed in the prediction of a solvatochromic shift. They can be applied to a crude estimation of the position of the absorption bands, but it requires systematic procedures for some empirical adjustment.

Relative Population of Radical Conformations. The primary aim of this work was to rationalize our previous experimental observation[23] of two kinetically distinct S∴O-bonded species, both absorbing in the 390 nm region, during the oxidation of (carboxyalkyl)thiopropionic acids by •OH radicals. A well-documented mechanism would require the calculation of transition states in solution, which cannot be achieved without an exceptional computational effort. However, on the basis of the computed free energies ΔG_s (see the last column of Table 1S) and λ_{max}, we can select the most stable conformations of **2** and **3**. Employing the Boltzmann equation[77] and the calculated ΔG_s values for the conformers of radical **2**, we derive their relative population as [**2A′**]:[**2B′**] ≈ 3:1. Similarly, for the protonated forms of radical **3**, we calculate a relative population of [**3DH′**]:[**3AH′**]:[**3CH′**] ≈ 3:2:1, showing that indeed different conformers of S∴O-bonded species may be formed simultaneously. Noticeably, the deprotonated structures **3A′** and **3D′**, which should absorb around $\lambda_{max} \approx 600$ nm, are not observed experimentally and can be excluded from our consideration. Thus, conformer **3B′** will be the almost exclusive (99%) form of the deprotonated radical **3**.

Conclusions

Combined DFT, semiempirical, and molecular mechanics methods give important information on possible structures and properties of S−O-bonded sulfuranyl radicals. Interpreted carefully, including useful correc-

(71) Asmus, K.-D. *Acc. Chem. Res.* **1979**, *12*, 436.
(72) Tomasi, J.; Perisco, M. *Chem. Rev.* **1994**, *94*, 2027.
(73) Cramer, C. J.; Truhlar, D. G. *Chem. Rev.* **1999**, *99*, 2161.
(74) Bayliss, N. S.; McRae, E. G. *J. Phys. Chem.* **1954**, *58*, 1002.
(75) Stevenson, D. P.; Coppinger, G. M.; Forbes, J. W. *J. Am. Chem. Soc.* **1961**, *58*, 4350.
(76) Rao, C. N. R. *Ultra-Violet and Visible Spectroscopy. Chemical Application*; Butterworth: London, 1975.
(77) Field, M. J. *A Practical Introduction to the Simulation of Molecular Systems*; Cambridge University Press: Cambridge, 1999; pp 1−313.

tions, our calculations allow reliable predictions for the properties of sulfuranyl species too large to accommodate in higher-level theoretical treatments, yet interesting due to their chemical and biological importance.

Acknowledgment. This work was supported by NIH Grant 2PO1AG12993. We thank Dr. Tomasz Wasowicz (Georgia State University), Dr. Janusz Rak (The University of Gdansk, Poland), and Dr. Ian Carmichael (Radiation Laboratory, The University of Notre Dame) for helpful discussions. D.P. thanks Prof. Jacqueline Bergés for kind introduction to the computational chemistry techniques during his visits to the Laboratorie de Chimie Théorique, Université P. et M. Curie, Paris, France.

Supporting Information Available: Computational methods, Tables 1S and 2S giving the basic structural changes and thermochemistry of solvation of the radicals and Mulliken spin distribution on the atoms involved in the S−O bond of model radical **4**, and Cartesian coordinates (Å) for the structures as well as total energies of the calculated radicals. This material is available free of charge via the Internet at http://pubs.acs.org.

JO010894L